

## Ion Energies at the Cathode of a Glow Discharge

W. D. DAVIS AND T. A. VANDERSLICE

*General Electric Research Laboratory, Schenectady, New York*

(Received 28 February 1963)

The energy distribution of ions striking the cathode in a glow discharge has been measured for a series of gases including hydrogen, helium, neon, and argon. Standard ultrahigh vacuum techniques were used to maintain a high degree of gas purity. The ions were detected by placing a small pinhole in the cathode of a glow discharge and analyzed for energy by means of a sector-type electrostatic analyzer. The ion species was determined with a conventional magnetic analyzer and the resulting ion beam intensity measured with an electron multiplier. An oscilloscope display gave the ion-energy distribution for a particular ion species. A simple theory involving assumptions that the ions originated in the negative glow and undergo primarily symmetrical charge transfer as they pass through the cathode dark space to the cathode gives results that are in most cases in good agreement with experiment. The charge-transfer cross sections determined are in reasonable agreement with other published data.

### INTRODUCTION

ONE of the important, but relatively unknown, quantities associated with a glow discharge is the energy distribution of the ions striking the cathode. A knowledge of this distribution would not only allow one to interpret more correctly the surface phenomena occurring at the cathode, but also should shed some light on the origins and life history of the ions traversing the cathode dark space.

In spite of the many experimental and theoretical investigations of glow discharges,<sup>1</sup> only limited success has been achieved in providing a detailed picture of the various phenomena occurring in the cathode fall region. It is generally agreed that electrons are created at the cathode and are accelerated by a linearly decreasing electric field across the dark space, that these energetic electrons cause ionization of the gas in the cathode fall and negative glow regions, and that some of the ions so produced arrive back at the cathode but there is no satisfactory quantitative description of these processes. To derive rigorously the energy distribution of the ions that strike the cathode, it would be necessary to know the relative amount of ionization occurring in the dark space as a function of distance from the cathode, the degree to which ions in the negative glow region diffuse out into the cathode fall region, and the cross sections and energy losses for the various collisional processes experienced by the ions as they are accelerated toward the cathode.

The first of these three parameters is in a primitive state of evolution. Some authors assume the motion of the electron is that of free fall and use the differential ionization coefficient to calculate the ionization in the cathode fall region. Others use the mobility concept and Townsend's first ionization coefficient  $\alpha$  in spite of the fact that these quantities apply only for homogeneous electric fields while the field of the cathode fall region is

strongly inhomogeneous, especially in the case of abnormal discharges. Recently Ecker and Müller<sup>2</sup> have calculated the motion of the electrons in the cathode fall region from the Boltzmann equation and the elastic and inelastic collision cross sections, but have not as yet used these results to determine the ionization distribution.

The role that the negative glow plays in supplying ions to the cathode fall region is also open to question. For example, Little and Von Engel<sup>3</sup> assume that none of the ions stem from the negative glow, while Scherzer<sup>4</sup> assumes that all the ions originate from the negative glow. From indirect evidence, Druyvesteyn and Penning<sup>1</sup> concluded that in the case of the normal glow a large fraction of the ionization occurred in the dark space while for abnormal discharges most of the ions came from the negative glow.

For the motion of the ions most theories assume that at any point they will have an average drift velocity determined by the mobility of the ions and the value of the electric field at that point. Thus, the average energy of ions striking the cathode would be determined by the field at the cathode irrespective of the source of these ions. However, the mobilities used are the steady-state drift velocities measured in a homogeneous electric field and would not be expected to apply for strongly inhomogeneous fields. In any case, the use of mobilities does not give the energy distribution of the ions, but only their average drift velocity.

Little and Von Engel<sup>3</sup> have calculated the average ion energy at the cathode by assuming that the only ion-molecule collisions that change the forward velocity of the ion are those of charge transfer. This is based on the fact that elastic collisions are predominantly small-angle scattering and thus do not affect the velocity of the ion to any great extent. Taking the average ion velocity to be that acquired over the last free path after a charge-

<sup>1</sup> Summaries may be found in G. Francis, in *Handbuch der Physik*, edited by S. Flügge (Springer-Verlag, Berlin, 1956), Vol. 22, p. 53; M. J. Druyvesteyn and F. M. Penning, *Rev. Mod. Phys.* **12**, 87 (1940); G. Ecker and K. G. Müller, *Tech. Report FTR 2 Co. No.: Da-91-591-EUC-1254*, 1961 (unpublished).

<sup>2</sup> G. Ecker and K. G. Müller, *Z. Naturforsch.* **16a**, 246-252 (1961).

<sup>3</sup> P. F. Little and A. Von Engel, *Proc. Roy. Soc. (London)* **A224**, 209 (1954).

<sup>4</sup> O. Scherzer, *Arch. Electrotechn.* **33**, 207 (1939).

transfer collision yields the following equation:

$$v = \left[ \frac{2eV_c}{M} \left\{ \frac{2\lambda}{pL} - \left( \frac{\lambda}{pL} \right)^2 \right\} \right]^{1/2},$$

where  $\lambda$  is the mean free path for charge transfer at  $p=1$  Torr,  $L$  is the length of the cathode fall region,  $V_c$  is the cathode fall potential, and  $M$  is the molecular weight.

The importance of charge transfer has been recently substantiated by Badereau *et al.*<sup>5</sup> From simultaneous measurements of the usual discharge parameters, they were able to calculate the collision cross section of the ions which agreed well with the published values for charge transfer obtained by other methods.

Experimental measurements of the ion energies at the cathode have been few and brief. None have involved separation and identification of the ions being measured nor have any used the modern high-vacuum techniques needed to ensure pure gases.

Chaudri and Oliphant<sup>6</sup> used a retarding field method and found that secondary electrons interfered with their measurements. Further experiments with an electrostatic analyzer were brief and leave much to be desired. Campan<sup>7</sup> later performed some simple experiments using a retarding field method. In both these cases, the study was not sufficiently extensive to give much understanding of the processes taking place in the discharge. No mass analysis of the various ion species was undertaken.

#### EXPERIMENTAL TECHNIQUES

The objective of the experimental work was to produce a glow discharge in a pure gas, withdraw a representative sample of the ions striking the center of the cathode and then determine the energy distribution of each species of ion with as little discrimination as possible. In addition, measurements of the cathode-negative glow distance as well as pressure, voltage, and current of the discharge were necessary.

The requirement of gas purity was attained by making the apparatus bakeable to 425°C. Hydrogen was obtained by diffusion through<sup>8</sup> Pd while the noble gases were "spectroscopically pure" gases in sealed glass bulbs. The ions were obtained by placing a small pinhole in the cathode of the glow discharge and then analyzed for energy by means of a sector-type electrostatic analyzer. The ion species was determined with a conventional magnetic mass analyzer and the resulting ion beam intensity measured with an electron multiplier.

<sup>5</sup> E. Badereau, I. Popescu, and I. Jova, *Ann. Physik* **5**, 308 (1960); E. Badereau and I. Popescu, *Rev. Phys., Acad. Rep. Populaire Roumaine* **5**, 41 (1960).

<sup>6</sup> R. M. Chaudri and M. L. Oliphant, *Proc. Roy. Soc. (London)* **A137**, 662 (1932).

<sup>7</sup> T. I. Campan, *Z. Physik* **91**, 111 (1934).

<sup>8</sup> J. R. Young, of this Laboratory, has analyzed H<sub>2</sub> purified in this manner and obtains an impurity level of less than 1 part per million.

Sufficient signal was obtained to display the complete energy spectrum of any one ionic mass on an oscilloscope.

A drawing of the main part of the apparatus is shown in Fig. 1. The discharge takes place in the central glass tube of about 6 cm diam. The cathode is a Kovar alloy spinning in the form of a hat with a crown 4.5 cm in diam and 2.5 cm high. A 1-cm-diam portion is gradually thinned out toward the center terminating in a small hole of about 0.1 mm diam.

For observing the discharge and measuring the dark-space distance, side ports with plane glass windows were added to the inner discharge tube and the outer steel can. Accurate measurements of this distance were difficult, especially for dark-space distances of a cm or more. For most cases, however, the error was probably no greater than 10%.

The ions after emerging from the pinhole are accelerated downward into the electrostatic analyzer. The first accelerating electrode consists of a disk with a  $\frac{3}{8}$ -in.-diam hole placed about  $\frac{1}{4}$  in. below the cathode. The second electrode is a cylindrical cage about  $1\frac{1}{4}$  in. diam. This electrode system evolved from several trials with other systems. The main difficulty was not in obtaining adequate intensity but rather in finding an arrangement which rapidly accelerated the ions away

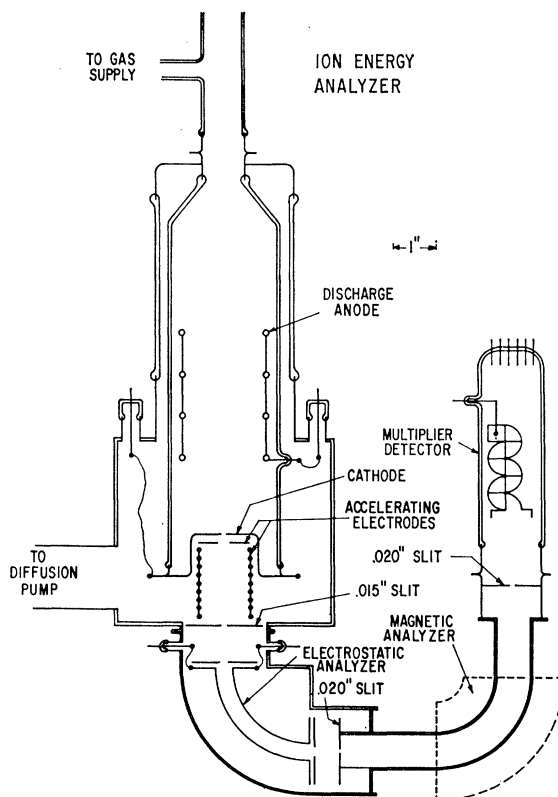


Fig. 1. Diagram of discharge tube and analyzers. Not shown are the windows in the discharge tube and outer can which allowed observation of the cathode fall region.

from the high-pressure region near the pinhole without preferentially focusing ions of any one energy onto the first slit. A satisfactory arrangement was considered to be one which did not significantly change the displayed energy spectrum as the voltages on the electrodes were varied over rather wide limits. After being accelerated, the spread in ion energy relative to the total energy is small and further discrimination effects were not noticed.

The electrostatic analyzer and magnetic analyzer are of conventional design. Both are  $90^\circ$  sectors with a 2-in. radius of curvature. With an entrance slit of 0.015 in. and an exit slit of 0.020 in., the energy spectrum from the electrostatic analyzer for an incoming ion beam of uniform energy spread should be a trapezoid with a base  $\Delta E/E$  of 1.75% and a flat top of 0.25%. The magnetic and electrostatic analyzer were designed to achieve double focusing and thus the combination should give perfect focusing for this small spread in energy. For any one mass, the beam at the final exit slit should then be 0.015 in. This slit was made 0.005 in. larger to accommodate the usual imperfections to be expected. A test of the completed analyzing section with a reasonably monoenergetic source of ions obtained by electron bombardment showed good agreement with these predictions as shown in Fig. 2. The theoretical mass resolution for adjacent masses is 57 and the ions of interest were easily separated.

The 10-stage electron multiplier was obtained from a commercial photomultiplier, Dumont No. 6467.<sup>9</sup> It was remounted as shown and after a bake out exhibited gains of  $10^6$ – $10^7$  for about 200–300 V/stage. The individual ion pulses could be easily observed. No accurate measurements of transmission losses were made but a typical discharge of about  $10^{-3}$  A gave about  $10^{-8}$  A of ion current through the pinhole and about  $10^{-10}$  A of resolved ion current at the multiplier input. With a multiplier gain of  $10^6$  and a 1-M $\Omega$  output resistor, this gave a signal of about 100 V on the oscilloscope. The background noise was no greater than 0.1 V and, thus, no trouble was experienced in observing small signals due to trace impurities or the rarer isotopes such as Ne<sup>21</sup>.

The lower end of the discharge tube is enclosed in a 5-in.-diam stainless steel vessel to which is attached a 2-in.-diam line leading to a bakeable alumina trap and 10-liter/sec oil diffusion pump. The capacity of this pumping system allowed one to maintain a pressure of about  $4 \times 10^{-5}$  Torr in the analyzing section for a pressure of 1 Torr in the discharge vessel. As pressures in the  $10^{-4}$  Torr region could be tolerated in the analyzing section, discharge pressures of several Torr could be achieved. The high-pressure section of the apparatus and the associated bakeable valves were evacuated with a liquid N<sub>2</sub> trapped mercury diffusion pump. After baking

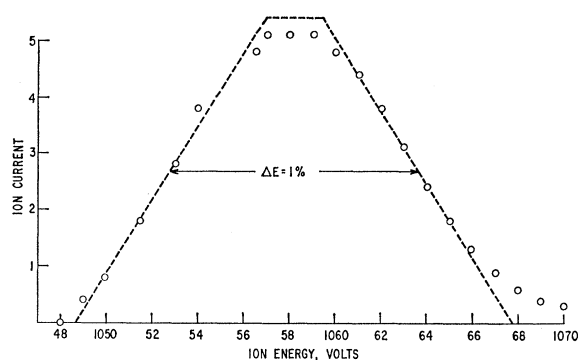


FIG. 2. Variation of the output from the electrostatic and magnetic analyzers as the accelerating voltage of a monoenergetic ion source is changed. The amplitude of the calculated curve has been adjusted to fit the  $\frac{1}{2}$  maximum points of the ion current curve.

out at  $425^\circ\text{C}$ , a base pressure of about  $10^{-9}$  Torr could be obtained in the apparatus.

Originally the pressure of the discharge was to be measured directly with a thermistor gauge but it was found that better results were obtained by reading the ion gauge present on the low-pressure side of the pinhole. This gauge was subsequently calibrated against a McLeod gauge temporarily attached to the high-pressure side.

For displaying the energy distribution of each ion species on an oscilloscope, equal but opposite polarity, constant voltages were applied to the electrostatic analyzer. This allowed only ions of a fixed energy (equal to 2.5 times the total voltage across the analyzer plates) to pass through the analyzer. A sawtooth-shaped voltage of about 1000 V peak superimposed on a constant positive potential of several kilovolts was applied to the cathode of the glow discharge. The peak potential of this modulated ion accelerating voltage was somewhat greater than that potential needed to give the ions emerging from the pinhole with zero velocity sufficient energy to pass through the electrostatic analyzer. Then by synchronizing the oscilloscope sweep with the sawtooth voltage and adjusting the magnet for the particular mass desired, the complete energy spectrum could be displayed. Other masses are displayed by simply changing the magnetic field. The sweep rate was in the range 10–100 cycles/sec.

Both accelerating electrodes were normally run at ground potential. This gives the maximum initial acceleration to the ions as they emerge from the pinhole. For low-discharge currents, the average potential between the first accelerating electrode and the cathode could be decreased by about  $\frac{1}{2}$  before there was any noticeable effect on the oscilloscope trace. At lower potentials, the intensity of the analyzed ion beam increased and the energy distribution changed markedly with small changes in potential. This implied that at the higher potential (highest initial acceleration), the accelerating system was not preferentially focusing any

<sup>9</sup> W. D. Davis and T. A. Vanderslice, in *Transactions of the Seventh National Vacuum Symposium, Cleveland, 1960*, edited by C. R. Meissner (Pergamon Press, Inc., New York, 1960), p. 417.

of the ions but indiscriminately defocusing all the ions and thus, a reasonably true picture of the energy distribution was being obtained.

**THEORY**

Before proceeding further, it would be desirable to develop the theory for the energy distributions that best describe our experimental observations.

It was noticed that the energy distributions obtained with various ions agreed qualitatively with the concept that charge transfer was the chief mechanism of energy loss. For example, symmetrical charge transfer between  $Ne^+$  and  $Ne$  has a higher cross section than does  $Ne^{++}$  and  $Ne$  and, indeed, the  $Ne^{++}$  ions have an average energy more nearly approaching their maximum energy than do the  $Ne^+$  ions. Argon is similar. It was also observed that, in those cases where charge transfer would be expected to be weak, a large proportion of the ions have an energy corresponding to the voltage across the discharge ( $H^+$  and  $H_2^+$  in  $He$  or  $Ne$ ). This suggests that, at least under some conditions, essentially all the ions come from the negative glow region.

Accordingly, the following model for the motion of ions in the cathode fall region was assumed:

1. All the ions originate in the negative glow or the very low-field region between the cathode fall and negative glow regions. For those cases where the mean free path for charge transfer is small compared to the dark space, it is only necessary that the ions originate several mean free paths away from the cathode so that essentially no ion is capable of drifting to the cathode without having at least one charge-transfer collision.

2. In those collisions responsible for the energy spectrum, the ion loses all its energy and the original ion, or the new ion formed, starts again from rest. This type of collision is probably dominated by symmetrical charge transfer in which an energetic ion interacts with its neutral counterpart producing a fast neutral and an identical ion with essentially zero energy. Charge transfer of this nature for which the  $\Delta E$  of reaction is zero are characterized by large cross sections as compared to unsymmetrical charge transfer or dissociation.

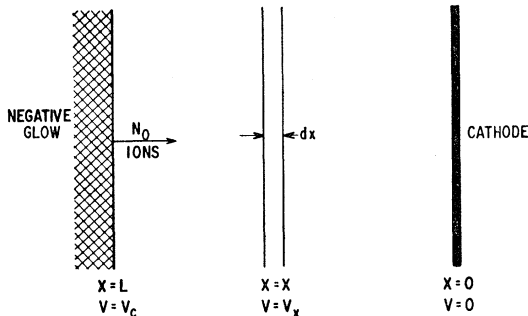


FIG. 3. Model used to derive energy distributions.

3. The cross section does not change with energy. The cross section for symmetrical charge transfer usually decreases with energy but for the range of ion energies of interest here, this decrease is sufficiently small to neglect.

4. The electric field decreases linearly from the cathode to the edge of the negative glow. Various investigators have shown this to be approximately the case.

The model used in the derivation of the energy distribution function is illustrated by Fig. 3. It is clear that the only way for an ion to reach the cathode with an energy corresponding to the potential  $V_x$  would be for

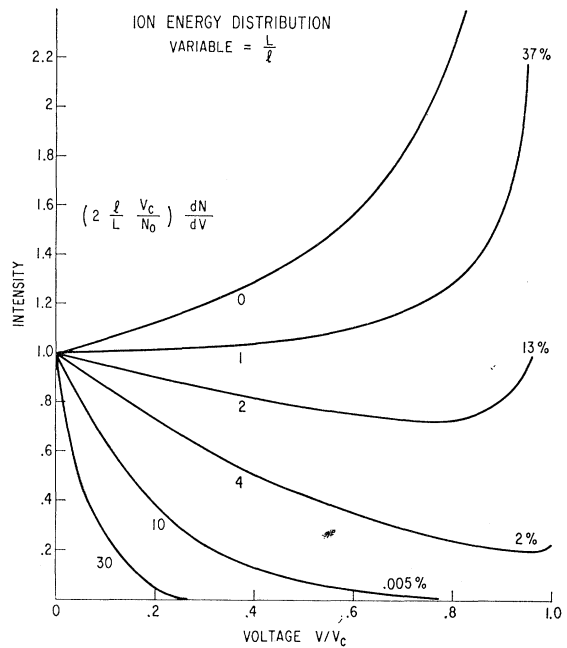


FIG. 4. Calculated energy distributions for various values of  $L/l$ . The percentages to the right refer to the proportion of ions which do not suffer any collision and would appear at  $V/V_c=1$ .

it to undergo charge transfer at point  $x$  and then travel all the way to the cathode without further collision. Taking the mean free path for charge transfer as  $l$  and noting that  $N_0$ , the number of ions starting from the negative glow, remains constant all the way to the cathode, the number of collisions that occur in the region  $dx$  would be  $N_0(dx/l)$ . The probability for any one of the resulting ions reaching the cathode without further charge transfer is given by  $e^{-x/l}$  and, thus, the number of ions of energy  $V_x$  at the cathode will be given by

$$dN = (N_0/l)e^{-x/l}dx. \tag{1}$$

Using the linear field relationship

$$x = L[1 - (1 - V_x/V_c)^{1/2}], \tag{2}$$

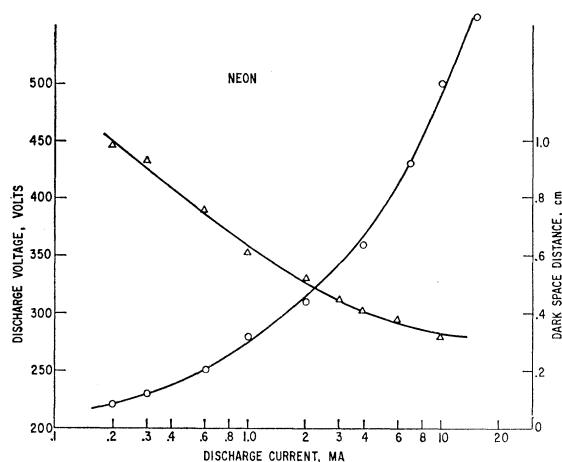


FIG. 5. Characteristics of a discharge in neon showing the normal behavior obtained in the experimental apparatus. Neon pressure was 1 Torr.

we arrive at the distribution function

$$\frac{V_c dN}{N_0 dV} = \left(\frac{L}{l}\right) \left[ \frac{1}{2(1 - V_x/V_c)^{1/2}} \right] e^{-(L/l)[1 - (1 - V_x/V_c)^{1/2}]} \quad (3)$$

This distribution is plotted in Fig. 4 for various values of  $L/l$ . It will be noted that the ions that do not suffer any collision but arrive at the cathode with the full cathode fall energy have not been included so far. Their relative number given by  $e^{-L/l}$  is indicated at the right end of the curves. The exact shape of this high-energy peak will of course depend on the instrumental resolution. For  $L \gg l$ , Eq. (3) reduces to an exponential relationship

$$\frac{V_c dN}{N_0 dV} = \frac{L}{2l} e^{-(L/2l)(V_x/V_c)} \quad (4)$$

#### EXPERIMENTAL RESULTS AND EXAMINATION OF THEORY

The gases used in the discharge were  $H_2$ , He, Ne, and Ar. The ions found in sufficient intensity to give good energy distributions were  $H^+$ ,  $H_2^+$ ,  $H_3^+$ ,  $He^+$ ,  $He_2^+$ ,  $Ne^+$ ,  $Ne^{++}$ ,  $Ar^+$ , and  $Ar^{++}$ . The presence of other ions could be detected, however. In addition, sufficient  $H_2$  was present as impurities in the noble gases to give the energy spectrum of  $H^+$  and  $H_2^+$  in these gases. The discharges used were all in the abnormal glow-discharge range although in most cases results could be obtained only slightly above the normal glow discharge condition. If the current was reduced sufficiently to obtain a normal glow discharge, the discharge was usually unstable and there was no assurance that the conditions immediately above the pinhole were representative of a normal glow discharge. In addition, the ion energies near the normal glow region were very low and could not be satisfactorily resolved. The currents used were

usually within the range  $10^{-4}$  A to  $10^{-1}$  A corresponding to approximately  $10^{-5}$ – $10^{-2}$  A/cm<sup>2</sup>.

The discharge pressures used varied from a few Torr to about 0.1 Torr. The highest pressure, as mentioned before, was primarily limited by the ability of the analyzing sections to function well at pressures greater than about  $10^{-4}$  Torr. In addition, the large currents involved at these higher pressures limited the study to low voltages where the ion energies were too low to measure accurately. The lowest pressure was limited by the available discharge voltage of about 750 V. Another consideration was the fact that at low pressures the dark space distance became too great to measure accurately through the windows of the apparatus.

The relationship between discharge voltage, current density, pressure, and dark-space distance were, within the experimental error, those to be expected for plane iron electrodes in the pure gas. This is shown in Fig. 5 for a neon discharge at approximately 1 Torr pressure.

The energy distributions obtained varied from ones having only ions of very low energy to ones having a large fraction of the ions at the maximum energy. For most ions, the distributions obtained were similar to the theoretical curves and, as the discharge current increased, the proportion of high-energy ions increased. The low-energy spectrums exhibited an exponential decay type of distribution which asymptotically approached the zero energy base line well short of the maximum energy. This is shown in Fig. 6 for  $H_2^+$  from a  $H_2$  discharge. As the proportion of higher energy ions increases, the tail of the exponential curve begins to be cut off at the maximum energy point, and a small peak of ions with this maximum energy usually can be seen (Fig. 15). With further increase in high-energy components, this peak grows and becomes the dominant feature of the distribution. In the case of  $Ne^{++}$  and  $Ar^{++}$ ,

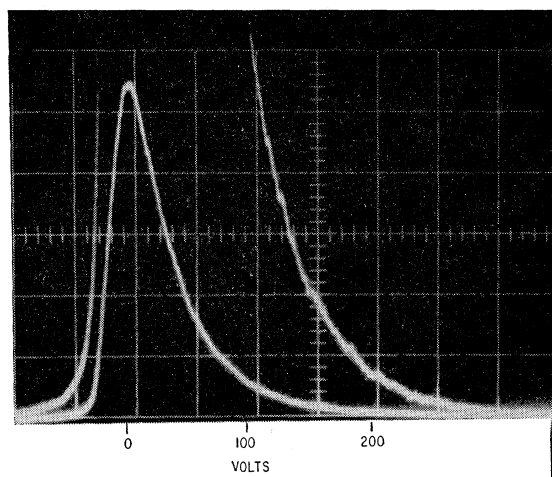


FIG. 6. Oscilloscope display of the energy distribution of  $H_2^+$  from a  $H_2$  discharge. The upper curve is a 10 $\times$  vertical expansion of the lower full curve. Conditions of discharge: 1.5 Torr, 440 V, 20 mA,  $L=0.61$  cm.

this whole sequence takes place as the current across the discharge is gradually increased and the dark-space distance decreases (Fig. 7). It will be noticed that the high-energy cutoff point increases with corresponding increases in the discharge voltage. From the magnitude of the sawtooth voltage applied to the cathode, the energy difference between the ions of minimum energy and those of maximum energy can be determined and in all cases, this energy difference agreed within experimental error with the voltage across the discharge.

Figure 7 also illustrates an apparent discrimination against low-energy ions that occurred for high-discharge currents. The intensity of the ions with energies below about 100 V was not that to be expected and more important, varied greatly with changes in the ion acceleration voltage and focusing voltages. With the focusing electrodes at ground potential, the discrimination pattern was the same for all ions, the maximum loss in intensity occurring at a few tens of volts ion energy rather than at zero energy. This effect was not serious for the  $H^+$  ion from  $H_2$  even for discharge currents of

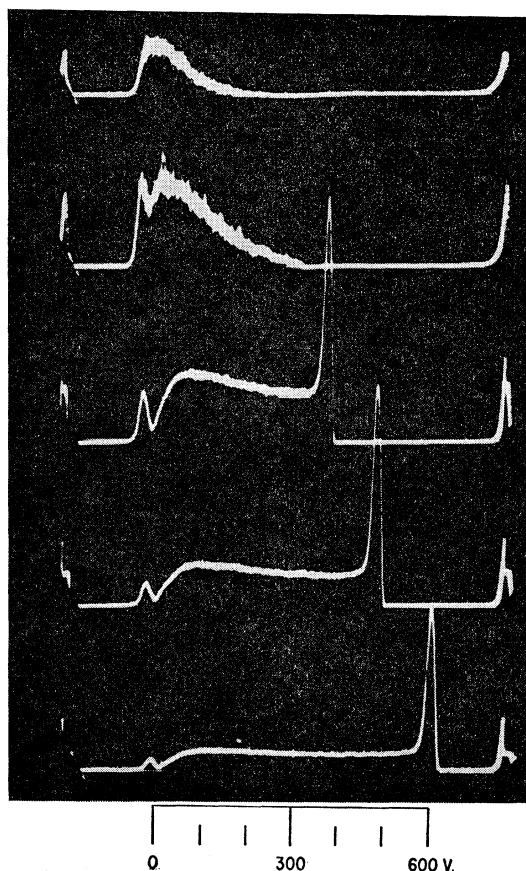


FIG. 7. Oscilloscope display of the energy distribution of  $Ar^{++}$  from an argon discharge. Discharge pressure = 0.5 Torr; discharge voltages (top to bottom) 300, 350, 400, 500, and 600 V; vertical sensitivity 0.05, 0.5, 1, and 2 V/cm. The discrimination at low ion energies causes the unusual shape at the left.

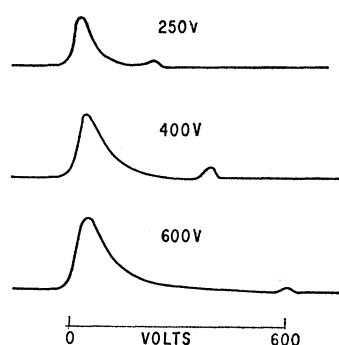


FIG. 8. Tracing of oscilloscope photographs showing energy distributions of  $He_2^+$  from a He discharge.  $p = 3$  Torr.

about 30 mA but the effect increased with mass as well as for current. Thus, for  $Ne^+$  from a Ne discharge, this discrimination became serious at about 5 mA. Increasing the accelerating voltage reduced the discrimination but even at 4000 V, it was still present. Higher voltages could not be used because of the decrease in energy resolution and the high magnetic fields needed for the higher masses.

The cause of this discrimination at high current could not be definitely ascertained. The fundamental difficulty, however, probably lies in the fact that the low energy ions, being formed near the cathode, are not well collimated as they emerge from the pinhole. Also they are easily influenced by space charges, charges on insulating surfaces, or stray magnetic fields. The high-energy ions, on the contrary, should be well collimated and much less disturbed by electric or magnetic fields. As a consequence, only the high-energy portion of the spectrum was considered of value under those conditions which showed discriminatory effects. Previous workers have not employed post acceleration techniques and in some cases<sup>6</sup> report maxima in the ion energy distribution. Probably the discrimination against low-energy ions gave rise to false maxima in their energy distributions for the reasons discussed above.

To test Eq. (3), points taken from the oscilloscope photographs are normalized and compared with the theoretical curves. In most cases, a good fit could be obtained for some particular value of  $L/l$ . From this value of  $L/l$  and measured values of  $L$  and the pressure, the collision cross section,  $\sigma$  can be calculated.

This experimental value of  $\sigma$  should not vary with variations in the conditions of the discharge such as pressure, current, and voltage. This was, indeed, found to be the case over the range used in this investigation. The final test of the theory is to compare these cross sections with the directly measured values for symmetrical charge transfer published in the literature.

#### $He^+$ and $He_2^+$

Energy distribution measurements on  $He^+$  were not possible because the ions had energies too low for satisfactory resolution. For example, at a pressure of 1.1 Torr and 500 V, the cathode fall distance was 1.0 cm. Using

$1 \times 10^{-15} \text{ cm}^2$  for the charge-transfer cross section for  $\text{He}^+$  and  $\text{He}$ ,  $L/l$  would be 40, a value too high for accurate resolution at normal acceleration voltages. For future measurements, this difficulty can be overcome by reducing the width of the slits in the electrostatic analyzer.

Ions were obtained at the mass 8 position which were assumed to be  $\text{He}_2^+$ . Their energy distributions as shown in Fig. 8 do not exhibit the same pattern as obtained with most other ions. The peak of high energy ions does not increase in intensity with decreasing  $L$  and is too large compared to the lower energy spectrum. The lower energy spectrum also does not change with decreasing  $L$  in the expected manner but, in fact, acts as if  $L/l$  were increasing. This distribution can be explained by assuming the  $\text{He}_2^+$  ions are formed in two places. The high-energy ions are undoubtedly formed in the negative glow and because there are few, if any,  $\text{He}_2$  molecules for charge transfer, they arrive at the cathode with the maximum energy. Some of these ions are undoubtedly lost by other types of inelastic collisions with  $\text{He}$  atoms but the results would not appear in the  $\text{He}_2^+$  spectrum. The lower energy  $\text{He}_2^+$  ions in the spectrum probably are formed within the dark space itself and their energy merely reflects the potential at which they were formed. One likely scheme by which the molecular ion might be formed would be for an excited  $\text{He}$  atom to interact with another  $\text{He}$  atom giving  $\text{He}_2^+$  and an electron.<sup>11</sup> The probability for excitation of  $\text{He}$  by electrons is a maximum in the neighborhood of 50 eV which agrees

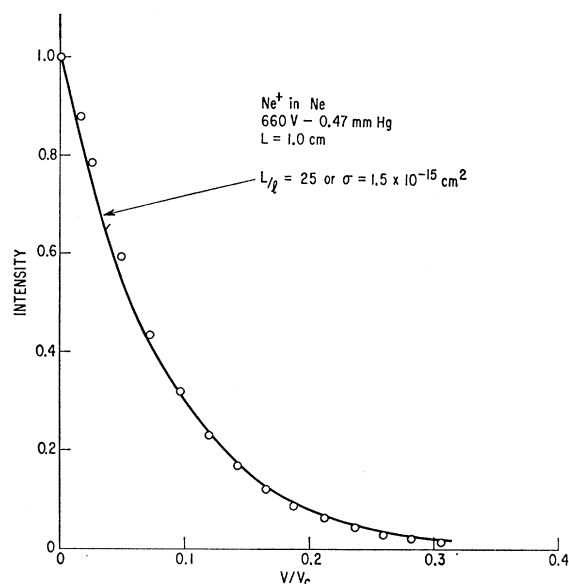


FIG. 9. Energy distribution for  $\text{Ne}^+$  from a  $\text{Ne}$  discharge. The circles are taken from an oscilloscope photograph and the full line is a theoretical curve fitted to the experimental points.

<sup>10</sup> W. H. Cramer and J. H. Simone, *J. Chem. Phys.* **26**, 1272 (1957).

<sup>11</sup> J. A. Hornbeck and J. P. Molnar, *Phys. Rev.* **84**, 615 (1951).

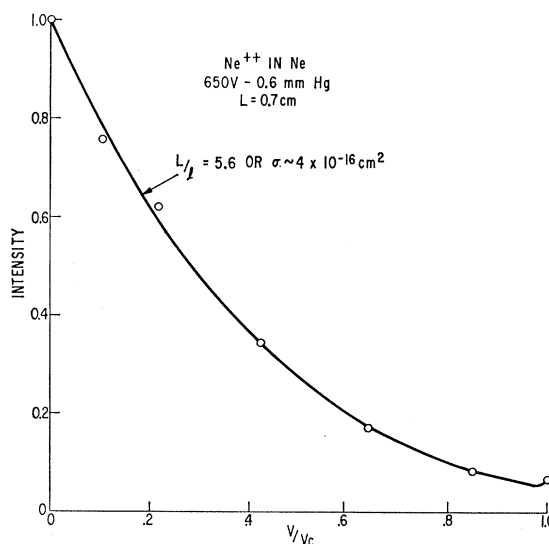


FIG. 10. Energy distribution for  $\text{Ne}^{++}$  from a  $\text{Ne}$  discharge. The full line is the calculated distribution that best fits the experimental points.

fairly well with the maximum in the energy distribution curve. A more detailed investigation of this ion is needed, however, before any firm conclusions can be drawn.

#### $\text{Ne}^+$ and $\text{Ne}^{++}$

Except for the low energy ions at high discharge currents, the energy distribution curves for these two ions agreed well with the theory. Figure 9 shows a curve for  $\text{Ne}^+$ . The calculated charge-transfer cross section for  $\text{Ne}^+$  and  $\text{Ne}$  of  $1.5 \times 10^{-15} \text{ cm}^2$  agrees remarkably well with the more direct measurements obtained by other investigations.<sup>12-15</sup> The cross section for  $\text{Ne}^{++}$  and  $\text{Ne}$  obtained from Fig. 10 is  $4 \times 10^{-16} \text{ cm}^2$ , while Wolf obtained a value of about  $3 \times 10^{-16} \text{ cm}^2$ .<sup>16</sup> Extrapolation of some recently published measurements at much higher energies indicate a cross section of  $5-10 \times 10^{-16} \text{ cm}^2$  in the energy range below 1000 V.<sup>13</sup>

#### $\text{Ar}^+$ and $\text{Ar}^{++}$

With argon, the ion energies are considerably shifted toward the higher energies and this case should have afforded a good test of the theory. However, the severe discrimination at high currents necessitated the use of only the low-current results for  $\text{Ar}^+$  as shown in Fig. 11. The cross-section value of  $5 \times 10^{-15} \text{ cm}^2$  is high compared to the directly measured values of Hasted.<sup>17</sup> He obtained

<sup>12</sup> H. B. Gilbody and J. B. Hasted, *Proc. Roy. Soc. (London)* **A238**, 334 (1956).

<sup>13</sup> I. P. Flaks and E. S. Solov'ev, *Zh. Tekhn. Fiz.* **28**, 599 (1958) [translation: *Soviet Phys.—Tech. Phys.* **3**, 564 (1958)].

<sup>14</sup> J. A. Dillon, *J. Chem. Phys.* **23**, 776 (1955).

<sup>15</sup> A. Rostagni, *Nuovo Cimento* **12**, 134 (1935).

<sup>16</sup> F. Wolf, *Ann. Physik* **34**, 341 (1939).

<sup>17</sup> J. B. Hasted, *Proc. Roy. Soc. (London)* **A205**, 421 (1951).

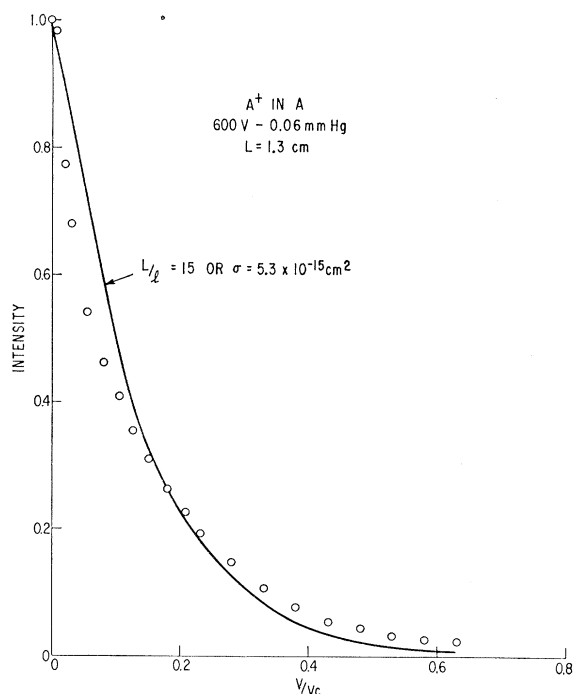


FIG. 11. Energy distribution for  $\text{Ar}^+$  from an argon discharge.

a value of about  $3 \times 10^{-15} \text{ cm}^2$  at 100 eV decreasing to  $2 \times 10^{-15} \text{ cm}^2$  at 600 eV. Similar results were obtained by other investigators.<sup>13,14</sup>

The energy distribution of  $\text{Ar}^{++}$ , as shown in Fig. 7, can be varied over a wide range. By choosing the last of this series, the theory can be tested for a case where  $L/l$  is low. The comparison is shown in Fig. 12 where

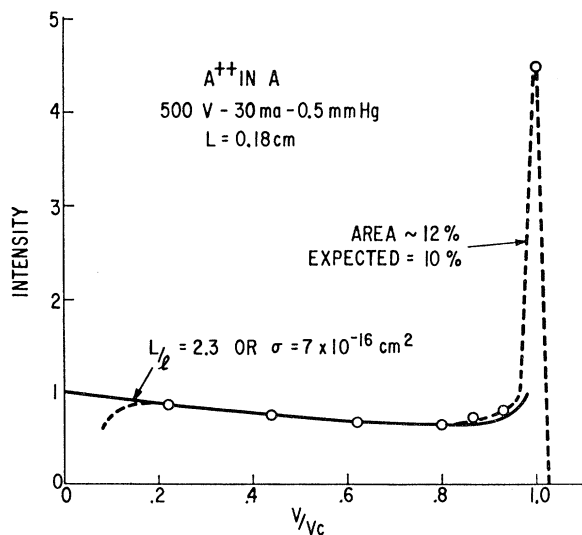


FIG. 12. Energy distribution for  $\text{Ar}^{++}$  from an argon discharge. Dashed line and circles are experimental values while full line is the calculated distribution for  $L/l=2.3$ . The area of the peak represents those ions with the full cathode fall potential.

agreement is good except, of course, for the low-energy end of the spectrum. Graphical integration of the high-energy peak yields a value for the proportion of full-energy ions in good agreement with the predicted value obtained by using the measured  $L/l$  value of 2.3. The charge transfer cross section of  $7 \times 10^{-16} \text{ cm}^2$  is somewhat low compared to Wolf's value of  $10 \times 10^{-16} \text{ cm}^2$ .<sup>16</sup> Extrapolation of Flaks and Solov'ev's<sup>13</sup> data at high energies yields an approximate value of  $10\text{--}15 \times 10^{-16} \text{ cm}^2$ .

### $\text{H}^+$ , $\text{H}_2^+$ , and $\text{H}_3^+$

Representative curves for these three ions in a  $\text{H}_2$  discharge are shown in Figs. 13, 14, 15;  $\text{H}^+$  always had the greatest proportion of high-energy ions and, as expected,  $\text{H}_2^+$  ions had the lowest energy distribution. No attempt was made at this time to obtain accurate measurements of the relative proportions of these ions but  $\text{H}_3^+$  and  $\text{H}^+$  predominate at pressures higher than about 1 Torr, while  $\text{H}_2^+$  predominates below this pressure.

The behavior of  $\text{H}_2^+$  agrees with that predicted by the model. As shown in Fig. 14, the shape of the distribution fits one of the theoretical curves quite well and the derived charge-transfer cross section of  $8.6 \times 10^{-16} \text{ cm}^2$  is reasonable. The published values range from about  $6 \times 10^{-16} \text{ cm}^2$  to  $8 \times 10^{-16} \text{ cm}^2$ ,<sup>12,14,18</sup> in the energy range of interest.

The distributions obtained for  $\text{H}^+$  are not so easily explained. One of the theoretical curves has been fitted to the experimental points of Fig. 13 even though it is

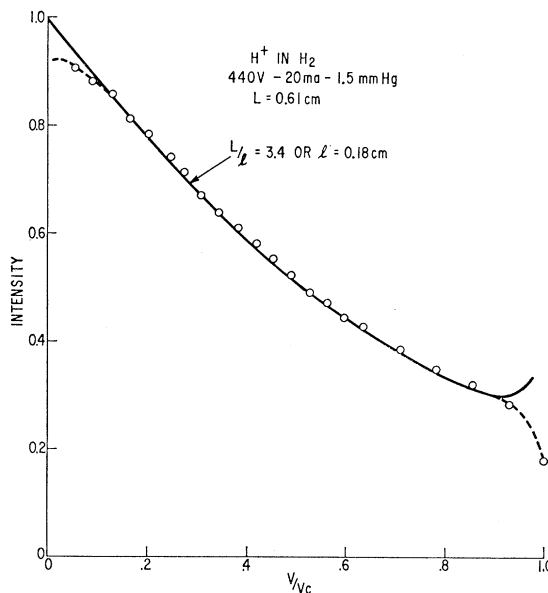


FIG. 13. Energy distribution of  $\text{H}^+$  in  $\text{H}_2$  compared with a calculated curve for  $L/l=3.4$ .

<sup>18</sup> J. H. Simons, C. M. Fontana, H. J. Francis, and L. G. Unger, *J. Chem. Phys.* **11**, 312 (1943).

not clear what process or processes are determining the energy distribution. If we assume for the moment that the significant reaction is charge transfer between  $H^+$  and  $H$  with a cross section of  $3 \times 10^{-16} \text{ cm}^2$ , the concentration of  $H$  atoms would have to be about 3% throughout the dark space.

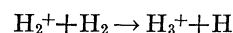
It is more likely that the distribution of  $H$  atoms is not uniform, the concentration being highest near the negative glow and decreasing towards the cathode. This would tend to increase the high-energy end of the distribution curve relative to the low-energy end, and thus would decrease the average  $H$  atom concentration needed to explain the results.

A nonuniform concentration of  $H$  atoms would also help to explain the fact that the peak of ions at the full cathode fall energy is missing. For example, if the  $H$  concentration were uniform, the distribution shown in Fig. 13 should have a prominent high-energy peak corresponding to about 3-4% of the total number of ions. Instead, a high-energy peak is barely discernible.

The energy distributions of  $H_3^+$  fit the theoretical curves very well (Fig. 15) but again, the collision processes responsible for the observed distributions are not known. For both  $H^+$  and  $H_3^+$ , variations in voltage and pressure of the discharge produce changes in the observed energy spectrum that one would expect if the

simple charge-transfer theory were valid and the mean free path was inversely proportional to the pressure. This suggests that the collision process involves the hydrogen molecule rather than any products of the discharge because the concentration of the latter would be expected to be strongly dependent on the conditions of the discharge. From Fig. 15, the cross section based on this assumption would be  $2.3 \times 10^{-16} \text{ cm}^2$  but unfortunately, little is known about the reactions of  $H_3^+$ . The high-energy peak is much larger than expected and corresponds to an  $L/l$  value of about 6.

There is considerable evidence that the reaction



has a large cross section of the order of  $5 \times 10^{-15} \text{ cm}^2$ .<sup>20-22</sup> This reaction could cause some of the  $H_3^+$  ions to be produced within the dark space but the main source of  $H_3^+$  should still be in the negative glow where the  $H_2^+$  and  $H_2$  would have more opportunity to react.

Varney<sup>21</sup> has deduced that the proton exchange

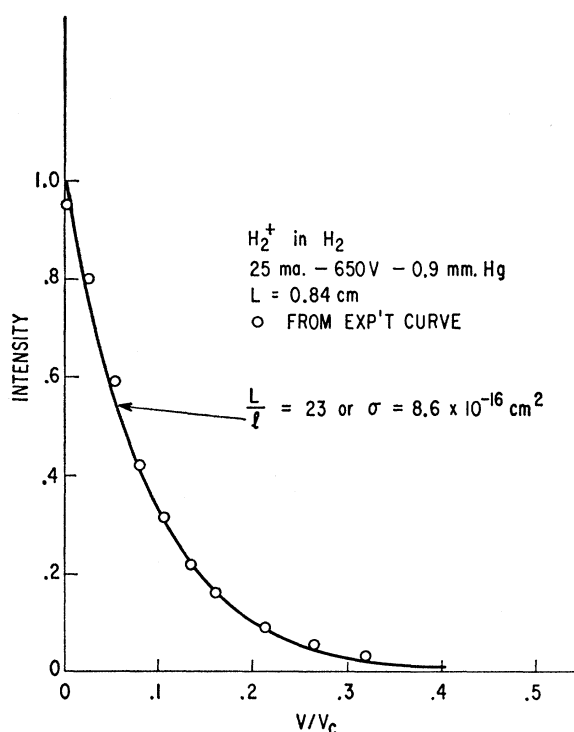


FIG. 14. Energy distribution of  $H_2^+$  from a discharge in  $H_2$ .

<sup>19</sup> W. L. Fite, *Proceedings of the Fourth International Conference on Ionization Phenomena in Gases, Uppsala, 1959* (North-Holland Publishing Company, Amsterdam, 1962), Vol. 1, p. IA-25.

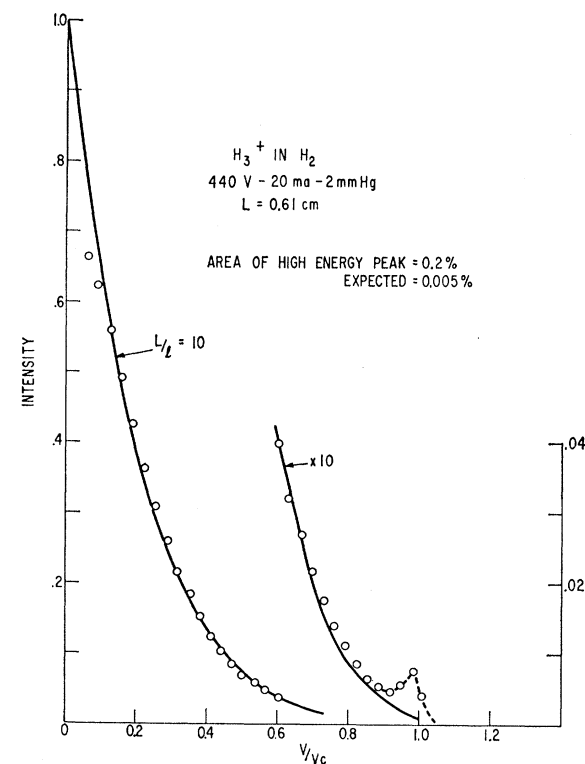


FIG. 15. Energy distribution of  $H_3^+$  from a discharge in  $H_2$ . The intensity scale for the right-hand curve has been expanded to show the high-energy components. A calculated curve based on the charge-transfer model has been fitted to the experimental points even though the specific collision processes are not known.

<sup>20</sup> W. S. Barnes, D. W. Martin, and E. W. McDaniel, *Phys. Rev. Letters* **6**, 110 (1961).

<sup>21</sup> R. N. Varney, *Phys. Rev. Letters* **5**, 559 (1960).

<sup>22</sup> D. P. Stevenson and D. O. Schissler, *J. Chem. Phys.* **29**, 282 (1958).

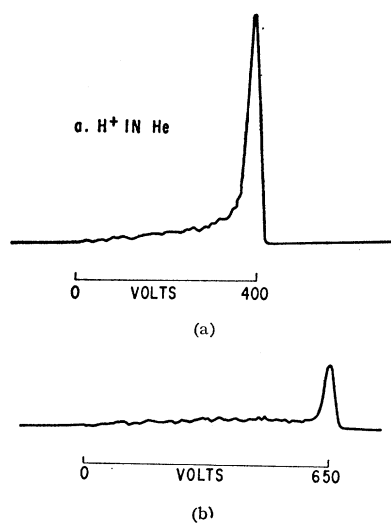
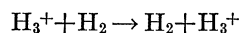


FIG. 16. Oscilloscope tracings showing the high ion energies obtained when charge transfer is greatly reduced by dilution. The  $H_2$  was present only as a trace impurity in the inert gas. No  $H_3^+$  was present. The maximum energy is approximately equal to the voltage across the discharge. (a)  $H^+$  in He; (b)  $H_2^+$  in Ne.

reaction



also has a large cross section of about the same magnitude. This reaction, of course, would directly affect the energy distribution but because the mass of the exchange proton is not negligible as is the mass of the electron in ordinary charge transfer, the analysis would be more difficult.

The analogous proton exchange reaction,



could be invoked to explain the  $H^+$  energy distribution but no data on this reaction are available.

For small amounts of  $H_2$  in another gas, there would be very little opportunity for  $H^+$  and  $H_2^+$  ions to undergo symmetrical charge transfer. In agreement with this, the energy distributions for  $H^+$  and  $H_2^+$  from small concentrations of  $H_2$  in Ne and He showed a large proportion of ions at the full energy as can be seen in Fig. 16. As in the case of pure  $H_2$ , the mean free path for  $H^+$  was greater than for  $H_2^+$ . The  $H_2$  was present as an impurity of unknown concentration and, thus, no quantitative interpretation of the results could be made. However, the shapes of the curves approximate the results to be expected for very small  $L/l$  except that the low-energy end of the curve falls off in intensity too

greatly. Quite possibly, when the opportunity for symmetrical charge transfer is greatly reduced, other types of collisions such as elastic collisions begin to play an important role in determining the energy distribution.

#### SUMMARY

This investigation has demonstrated that the ions striking the cathode of a glow discharge have a wide range of energies ranging up to that corresponding to the full cathode fall of potential. The determining factor for each ion species appears to be the ratio between the mean free path for symmetrical charge transfer with ambient gas molecules and the cathode dark-space distance. When the mean free path is relatively large, many of the ions manage to traverse the cathode dark space with little or no collisions and thus the high energies predominate. When the mean free path is small, most of the ions have their last collision close to the cathode and the ion formed by the symmetrical charge transfer process cannot regain much energy before hitting the cathode. For constant discharge voltage, the effect of gas pressure on the energy distribution is small. This is explainable on the basis that in a glow discharge the product of pressure and dark-space distance is relatively constant and thus the average number of collisions per ion in traversing this distance is constant. If the pressure is kept constant, increasing the voltage (or current) decreases the dark-space distance and the proportion of high energy ions increases.

For normal glow discharges, the mean free path for charge transfer is small compared to the dark-space distance and thus the very low-energy ions predominate. The energy distribution of these ions is essentially independent of whether they originate from the negative glow or merely several mean free paths from the cathode. The higher energy ions are too low in intensity to satisfactorily resolve their distribution in energy. As a result, the origin of the ions in normal glow discharges cannot be deduced.

For abnormal discharges, the energy distribution of most ion species can be quantitatively explained in terms of the simple model. This strongly indicates that the ions originate predominantly in or near the negative glow and lose energy chiefly through charge transfer. The energy spectra of  $H^+$  and  $H_3^+$  are not so simply explained and further work will be needed to elucidate the processes responsible for them.

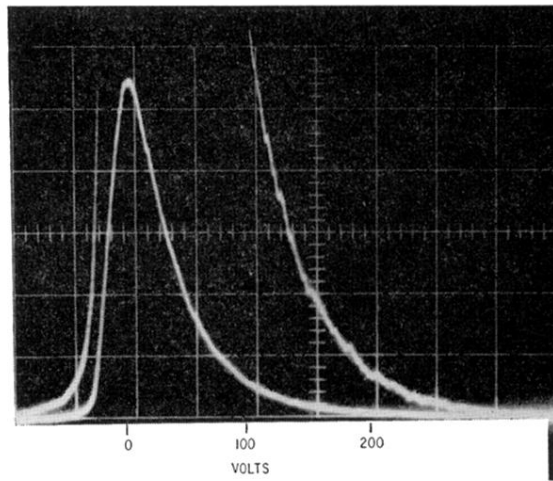


FIG. 6. Oscilloscope display of the energy distribution of  $\text{H}_2^+$  from a  $\text{H}_2$  discharge. The upper curve is a  $10\times$  vertical expansion of the lower full curve. Conditions of discharge: 1.5 Torr, 440 V, 20 mA,  $L=0.61$  cm.

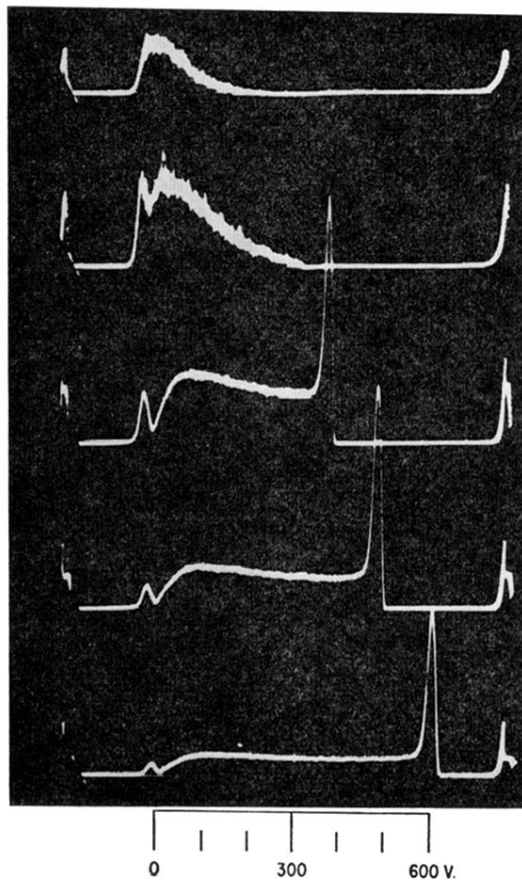


FIG. 7. Oscilloscope display of the energy distribution of Ar<sup>++</sup> from an argon discharge. Discharge pressure=0.5 Torr; discharge voltages (top to bottom) 300, 350, 400, 500, and 600 V; vertical sensitivity 0.05, 0.5, 1, and 2 V/cm. The discrimination at low ion energies causes the unusual shape at the left.